

Washington University in St. Louis

Washington University Open Scholarship

Mechanical Engineering and Materials Science
Independent Study

Mechanical Engineering & Materials Science

12-21-2016

MOUDI analysis of particle size distributions for ultrasonic spraying of salt solutions from an array of microscopic orifices

Yichen Sun

Washington University in St. Louis

J. Mark Meacham

Washington University in St. Louis

Follow this and additional works at: <https://openscholarship.wustl.edu/mems500>

Recommended Citation

Sun, Yichen and Meacham, J. Mark, "MOUDI analysis of particle size distributions for ultrasonic spraying of salt solutions from an array of microscopic orifices" (2016). *Mechanical Engineering and Materials Science Independent Study*. 32.

<https://openscholarship.wustl.edu/mems500/32>

This Final Report is brought to you for free and open access by the Mechanical Engineering & Materials Science at Washington University Open Scholarship. It has been accepted for inclusion in Mechanical Engineering and Materials Science Independent Study by an authorized administrator of Washington University Open Scholarship. For more information, please contact digital@wumail.wustl.edu.

MOUDI analysis of particle size distributions for ultrasonic spraying of salt solutions from an array of microscopic orifices

Yichen Sun, yichensun@wustl.edu

Washington University in St Louis, Department of Mechanical Engineering and Material Science

Abstract: We report characterization of spray-based nanoporous particle synthesis for use in the cathode of lithium-ion batteries. Ultrasonic Microarray Spray Tuning (uMIST) was used to create microdroplets of salt solutions and battery material precursors, and the size distributions of produced microdroplets were investigated with a Micro-Orifice Uniform Deposit Impactor (MOUDI). Experimental challenges associated with spray orientation, flow control and consistency of operation were addressed, and a promising solution for continuous droplet collection to obtain a statistically relevant droplet size distribution was proposed. Improved analysis capabilities will lead to a better understanding of the uMIST droplet formation mechanism.

Keywords: Ultrasonic droplet generation, Drop-on-Demand, Spray Pyrolysis, MOUDI

Introduction

Lithium-ion batteries stand out for their significant energy density, inherent design flexibility and long lifespan, but their development has been historically slowed by complications in designing suitably functional material interfaces.^[1] Fergus^[2] provides a thorough review of recent developments related to lithium-ion battery cathode materials including discussion of different chemistries and the effect of microstructure and morphology. It is shown that nanoporous microscale particles are desired to give high surface area to volume ratio, short diffusion distances characteristic of small particles (hundreds of nanometers), controllable electrode reactivity and simple handling. Spray pyrolysis can create such particles; however, aerosol sources typically yield hollow and deformed spheres when secondary particles are larger than approximately 2 μm .^[4] The final size of nanoporous particles produced using ultrasonic Microarray Spray Tuning (uMIST) depends on the diameter of the droplets from which the particles are formed. This relationship is illustrated in Fig. 1. To avoid reduced performance associated with hollow particles, a precursor droplet diameter of less

than 10 μm is required.^[3] In this report, we assess uMIST capabilities for battery cathode material production by attempting to relate a droplet formation mechanism (and resulting droplet size distribution) to specific device operating conditions.

I. Droplet-on-demand

For nozzle-based drop-on-demand droplet generation, droplet radius R_d is typically of the same order as the radius R of the nozzles that produce them.^[5] Numerous techniques exist for making drops with radii much larger than that of the nozzles;^[6,7] however, the only reliable means to achieving a decreased drop volume has been to reduce the orifice size.^[5]

Contrary to this accepted restriction on droplet size, we have observed generation of a mist of small droplets ($<10 \mu\text{m}$) using a uMIST with 17 and 55 μm nozzle orifices.^[3] Thus, the physical mechanisms underlying spray generation by uMIST are of interest.

uMIST comprises a PZT-8 piezoelectric transducer, an optional aluminum coupling layer and a sample chamber bounded by a silicon nozzle microarray (see Fig. 2). Figure 3 shows a working uMIST, along with high-resolution SEM images of the pyramidal nozzle geometry.

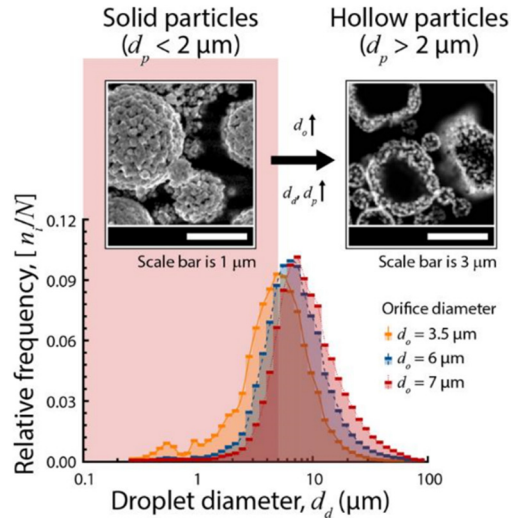


Figure 1 Hollow particle formation condition

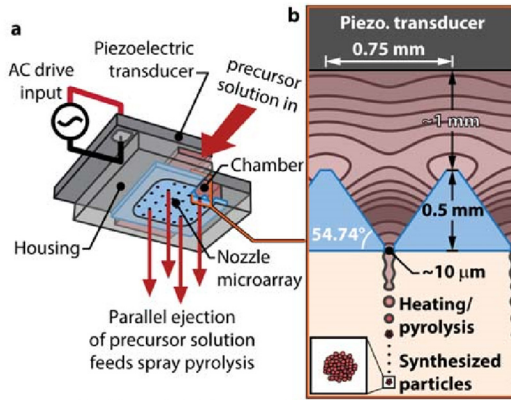


Figure 2 (a) 3D illustration of uMIST components, (b) detail of representative nozzle geometry

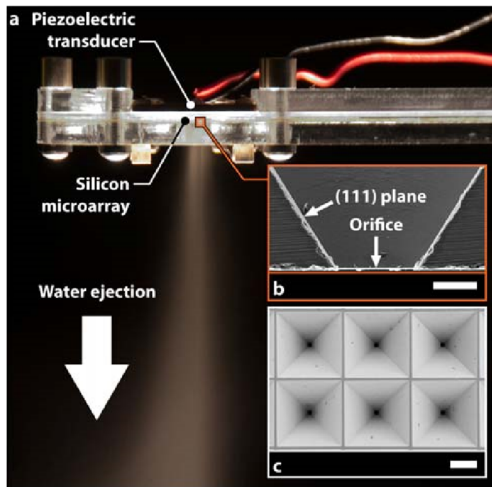


Figure 3 (a) uMIST during operation, (b/c) SEM images of the nozzle geometry

The silicon nozzles are formed using a simple batch microfabrication process that involves wet etching of (100) silicon in potassium hydroxide solution. [8] The thickness of the piezoelectric is chosen so that its longitudinal resonance is within an envelope of desired cavity resonances. [8] When the piezoelectric transducer is driven by the amplified signal of a standard function generator at particular resonant frequencies of the fluid chamber, constructive interference due to the shape of the pyramidal structure focuses acoustic waves towards the nozzle orifices. A standing acoustic wave develops with its peak pressure gradient occurring near the tip of the nozzle, which counteracts surface tension and viscous forces to eject microdroplets.

II. Spray pyrolysis

In conventional spray pyrolysis, an aerosol of precursor solution is conveyed into a heated reactor where the solvent evaporates, solutes precipitate, and decomposition reactions form product particles. [9] For the spray characterization work described here, we eject precursor solutions upward into a heated tube to evaporate solvent (water). Due to a chimney effect, light solute particles flow upward and are pulled into a MOUDI system under vacuum for determination of the particle (and thus droplet) size distribution.

III. Salt solution simulation

Because battery precursor solutions decompose at just slightly higher than 60 °C, we use salt (calcium chloride and sodium chloride) solutions to simulate the spraying behavior of battery precursor solutions. The acoustic pressure field within the nozzles (and thus the pressure gradient at the nozzle tips) is a function of operating frequency, which in turn is dependent on the speed of sound (SOS) of the working fluid. To model the spraying behavior of uMIST loaded with five different concentrations of battery precursor, different concentrations of salt

solutions (CaCl_2 and NaCl) were prepared such that the SOS in these solutions matched that of the corresponding battery precursor solutions. Salt solutions were prepared in different concentrations based on their reported speeds of sound, and the setup shown in Fig. 4 was used to verify the SOS data. In this system, two ultrasonic transducers are connected to a pulser-receiver unit and oscilloscope. The sample to be measured is then loaded between the two transducers. Matlab computes the SOS for a given sample by comparing a pulse wave sent from the transmitting transducer and the waveform recorded by the receiver. A typical pair of incident and received signals is shown in Fig. 5. ^[10]

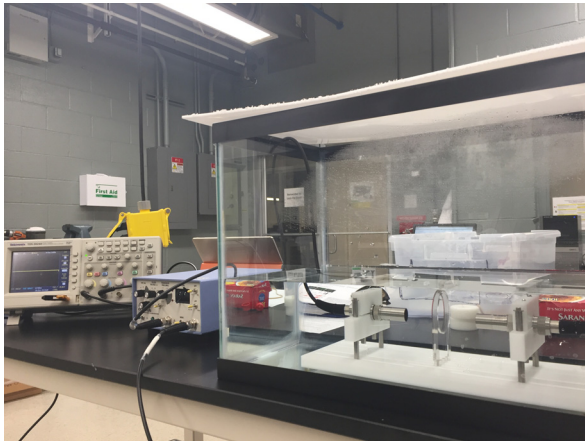


Figure 4 Speed of Sound (SOS) testing setup

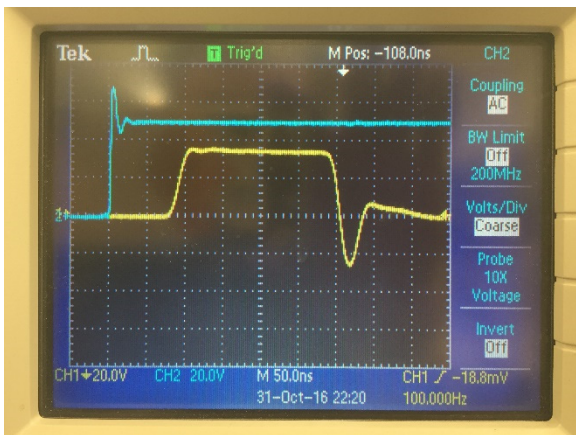


Figure 5 Incident (Blue) and received (Yellow) signals in SOS testing

IV. MOUDI System

Figure 6 shows the system used to analyze the droplet size distribution. The closed assembly of metal discs on the right is a MOUDI, in which 11 stages are designed to collect particles from $<1 \mu\text{m}$ to $10 \mu\text{m}$. Particles are pulled into the system by a vacuum pump (the blue box of Fig. 6), with flow regulated by a needle valve and rotameter.

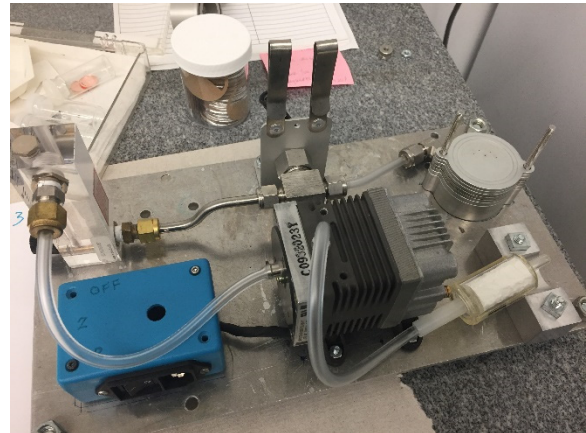


Figure 6 MOUDI system

Methods and Experiment

I. uMIST Testing

Initial characterization of a new uMIST device used deionized (DI) water as the working fluid. Nozzle microarrays were adhesively mounted in a two-part milled polycarbonate housing. Multiple orifice sizes ranging from 17 to $65 \mu\text{m}$ were investigated. After assembly of the plastic components, a 1.5 mm piezoelectric and 3 mm -thick aluminum coupling layer (1 mm embedded in housing, 2 mm coupling piece) were attached using stainless steel clips. Two drops of DI water were applied between each transducer layer to ensure good acoustic contact between surfaces, and electrical connections were made. Optimal spraying conditions (e.g., input signal frequency, Peak-Peak voltage, power forward and power reflected, and

operating temperature) were identified and recorded while scanning the drive frequency.

II. Salt solution preparation

Five aqueous calcium chloride solutions were prepared to match SOS data obtained from previous testing of 0.5, 1, 2.5, 4, and 8 mol/L battery precursor solutions. Concentrations shown in Table 1 were based on reference data from the literature. [11]

Table 1 Preparation of CaCl₂ solutions (50 ml)

CaCl ₂ Molality (mol/kg)	Theoretical CaCl ₂ (g)	Experimental CaCl ₂ (g)
0.3	1.79	1.8342
0.55	3.2817	3.281
1.35	8.055	8.053
2.27	13.544	13.546
6.53	38.962	38.964

Table 2 Comparison of Speed of Sound between prepared salt solutions (Right) and precursor solutions (Left)

Molarity (mol/L)	BP SOS (m/s)	Molality (mol/kg)	CaCl ₂ SOS (m/s)
0.5	1512.8	0.30	1519.9
1	1544.3	0.55	1537.6
2.5	1596.3	1.35	1602.5
4	1682	2.27	1667.4
8	1834.6	6.52	1840.5

Table 1 summarizes the solutions of calcium chloride (Sigma-Aldrich, MW:110.98, Anhydrous Granular ≤ 7.0 mm, purity $\geq 93\%$) used in testing, 0.3, 0.55, 1.35, 2.27 and 6.53 mol/kg. Table 2 compares reported SOS of prepared CaCl₂ solutions and corresponding battery precursor solutions. SOS of prepared samples were validated using the SOS Testing System of Fig. 4. Unfortunately, all calcium chloride solutions exhibited a smoky sediment, indicating undesirable dissolution. To address this issue, a 0.5 mol/L sodium chloride solution was also prepared.

III. Determination of particle size distributions

uMIST was modified to spray upward as shown in Fig. 7. In this orientation, inlets and outlets were sealed to syringes. A syringe was loaded with solution and connected to the inlet. The contents of the loading syringe were dispensed into the cartridge reservoir and an open syringe connected to the reservoir outlet. The syringe connected by tube to the outlet was held such that a balance was reached between the hydrostatic pressure in the open syringe and the atmospheric pressure at the nozzles. In this way, the system could be continuously loaded from the open syringe to maintain spraying.

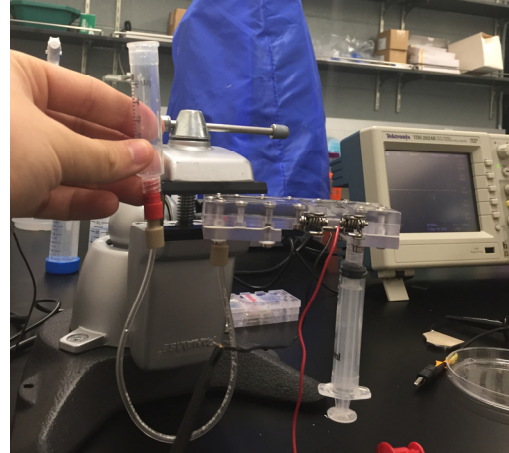


Figure 7 Modified uMIST device for spraying upward

As shown in Fig. 8, the assembled uMIST device was placed at the bottom of a heated aluminum tube. (lower left corner). The aluminum tube was wrapped with temperature-adjustable heating tape and covered with insulation materials. The heated air inside the tube was measured to be 120 °C, and the MOUDI system was placed at the outlet of the heated aluminum tube for collecting salt particles. uMIST was operated in a burst mode, spraying for 1.5 seconds and pausing for 1.5 seconds until all solutions were sprayed. When spray was started, a laser beam was used to check the outlet of the aluminum tube for exiting particles. When

reflected particles were observed, a blank paper was placed near the outlet to check if all liquid water was evaporated. The MOUDI was then set to collect sample at a flow rate of 4 cm³/s.



Figure 8 Connected droplet evaporation testing system

After the collection was completed, the MOUDI was disassembled and each of the 11 impaction plates were weighed three times to obtain an average value.

Results and Discussion

The optimal operating frequencies and other parameters for spraying of DI water with different reservoir heights are shown in Table 3.

Table 3 Spraying conditions for uMIST with different reservoir heights

H	Freq (Hz)	Voltage (V)	Pf (W)	Pr (W)	Temp (°C)
0.9	860k	194	41	32	26.2
	1.25M	126	40	25	28.2
	1.65M	216	43	27	26.2
1.0	2.20M	208	80	68	26.6
	770k	188	32	27	25.5
	1.18M	92	13	8	24.5
	1.52M	104	20	1	25.5
	2.03M	210	64	51	25.4

1.1	690k	162	23	19	23.2
	1.13M	57.6	5	3	24.6
	1.45M	67.2	14	0	26.6
1.2	1.92M	256	82	73	25.6
	680k	256	60	50	22.3
	1.07M	92	12	8	24.4
	1.37M	92	53	28	26.8
1.3	1.78M	224	54	45	25.8
	600k	172	23	20	24
	1.01M	82	8	5	24.3
	1.33M	120	63	25	26.9
	1.67M	112	11	6	25

As shown in Tables 1 and 2, calcium chloride solutions were prepared such that the solution SOS matched with those of previously tested battery precursor solutions. This ensured that salt solutions behaved similarly from an acoustics perspective and that the determining factor for spraying or not from a given reservoir geometry at a particular frequency of operation was identical.

Unfortunately, calcium chloride was not easily dissolved for unknown reasons, which could adversely affect device operation. For this reason, we transitioned to testing with an aqueous sodium chloride solution at 0.534 mol/L.

As we were attempting to test the particle size distribution from a uMIST device after droplet evaporation, larger droplets containing more solutes result in larger salt particles, while small misting droplets become smaller salt particles. Therefore, there is a correlation between droplet size distribution from the ejector and particle size distribution after evaporation (or pyrolysis of the battery precursors). After modification of the existing uMIST for upward spraying, the ejector robustly worked for about 5 minutes; however, its performance decreased significantly as crystallized salt began to appear around the edges of the silicon nozzle microarray. This is likely due to heating from

the evaporation tube, which could also heat the piezoelectric transducer, shifting the frequency of operation. Either or both of these observations could be detrimental to device operation and may explain the relatively short-lived spraying. Nonetheless, the 11 stages were weighed after 5 minutes of collection, and the results are shown in Table 4.

Table 4 MOUDI collection results

Stage Number	Weight
1	0.02916
2	0.02946
3	0.02913
4	0.02923
5	0.02952
6	0.02923
7	0.02954
8	0.02944
9	0.02934
10	0.02949
11	0.02929
Average	0.02935

The data suggest that there is no significant increase in the weight of any impaction plate. This may be explained by the relatively small area of the collection tube in comparison with the overall evaporation tube outlet. If only 1% of the total 10 ml sprayed solution was collected, a rough estimation of expected recovery suggests that a total increase of 0.003 g is expected. The average MOUDI plate weight prior to testing was 0.0292 g. The estimated total weight increase corresponds to only a 0.0003 g increase in weight if averaged across each impaction plate. Even this likely produces a high estimate as some spray impacts on the evaporation tube inlet and inner surfaces. Regardless, the results above suggest that no, or at least very few, particles were collected.

Conclusions and Future Work

Although our results indicate that too few particles were collected to complete an effective analysis of the droplet size distribution from a uMIST device, we see a great potential to complete and improve our current experiment. Higher concentration salt solutions will be used to ensure sprayed particles are large enough to be detected across multiple plates. A higher flow rate at the impactor system inlet will be more likely to extract particles from the outflow. Finally, a larger conical inlet will be added to the MOUDI system.

Working temperature will be more closely monitored for the uMIST device because higher temperatures are detrimental to the performance of the piezoelectric transducer. To address potential heating issues, the distance between the uMIST outlet and the evaporator tube inlet will be increased to reduce the chance of salt crystallization on the nozzle microarray.

Acknowledgements

I would like to give special thanks to Dr. Meacham who helped me throughout the project and shared much precious research experience with me. I would also like to thank Michael Binkley, Minji Kim, and Mike Shen. They gave me invaluable help in setting up my devices and completing my project.

References

- [1] Armand, Michel, and J-M. Tarascon. "Building better batteries." *Nature* 451.7179 (2008): 652-657.
- [2] Fergus, Jeffrey W. "Recent developments in cathode materials for lithium ion batteries." *Journal of Power Sources* 195.4 (2010): 939-954.

- [3] Champlin, Patrick A., and J. Mark Meacham. "Characterization of Ultrasonic Precursor Solution Spraying for Battery Material Synthesis." (2016).
- [4] Meacham, J. M., 2015, "I-CARES Project Description," (150311).
- [5] Le, Hue P. "Progress and trends in ink-jet printing technology." *Journal of Imaging Science and Technology* 42.1 (1998): 49-62.
- [6] Lee, Francis C., Ross N. Mills, and Frank E. Talke. "Drop-on-demand method and apparatus using converging nozzles and high viscosity fluids." U.S. Patent No. 4,475,113. 2 Oct. 1984.
- [7] Self, Roger G., and David B. Wallace. "Method of drop size modulation with extended transition time waveform." U.S. Patent No. 6,029,896. 29 Feb. 2000.
- [8] Meacham, J. M., et al. "Micromachined ultrasonic droplet generator based on a liquid horn structure." *Review of Scientific Instruments* 75.5 (2004): 1347-1352.
- [9] Gurav, Abhijit, et al. "Aerosol processing of materials." *Aerosol science and technology* 19.4 (1993): 411-452.
- [10] Chintapalli, Sreyas, and J. Mark Meacham. "Design, Fabrication, and Programming of an Acoustic Property Measuring System for Ultrasound in the MHz Range." (2016).
- [11] Wahab, Abdul, and Sekh Mahiuddin. "Isentropic compressibility and viscosity of aqueous and methanolic calcium chloride solutions." *Journal of Chemical & Engineering Data* 46.6 (2001): 1457-1463.